Geological Survey of Japan Cruise Report No. 20, p. 67–89, 1984

VII. DEEP-SEA SEDIMENTS IN THE GH80–5 AREA IN THE NORTHERN VICINITY OF THE MAGELLAN TROUGH

Akira Nishimura

Introduction

Lithologies of the sediment samples collected during the GH80–5 Cruise are described, and an attempt to construct the sedimentary history of the surveyed area is made on the data of the lithologic features, combined with the paleontological and paleomagnetic studies of the sediment samples, in this chapter.

In this cruise, close samplings were performed in the two small areas to clarify local variations in abundance and morphology of manganese nodules, and the corresponding sediment distributions and sedimentary sequences. Sediment and manganese nodule samplings were performed by the following methods.

*Double-spade box corer at 24 sites
*Piston corer with a barrel of 8 meter long at 17 sites
*Freefall grab with a small sediment sampling tube at 68 times
*Dredge at 3 sites

Bottom sediments sampled by a box corer and a piston corer were handled through the same process as the previous work (NISHIMURA, 1981). Color determination of sediments was based on the system of "Munsell Soil Color Chart". Lithologic types of sediments were determined by smear slide observations. The components distinguished under the microscope using smear slides are as follows.

*Biogenic components

1.	foraminifers (planktonic)	(calcareous)
2.	calcareous nannoplanktons	(calcareous)
3.	diatoms	(siliceous)
4.	radiolarians	(siliceous)
5.	sponge spicules and radiolarian spines	(siliceous)
6.	silicoflagellates	(siliceous)
7.	ichthyoliths	(phosphatic)

*Authigenic components

8.	zeolite minerals	
9.	manganese micronodules	

*Miscellaneous components

10.	carbonate unspecified possible fragments of foraminiferal tests	(calcareous)
11.	clay	

Table VII-1. Framework of sediment type classification.

PELAGIC CLAY *zeolite, siliceous fossil, and calcareous fossil*<5%		
ZEOLITE RICH CLAY 5%<*zeolite*<10%	SILICEOUS FOSSIL RICH CLAY 5%<*siliceous fossil*<10%	CALCAREOUS FOSSIL RICH CLAY 5%<*calcareous fossil*<10%
ZEOLITIC CLAY 10%<*zeolite*	SILICEOUS CLAY 10%<*siliceous fossil*<30%	CALCAREOUS CLAY 10%<*calcareous fossil*<30%
	SILICEOUS OOZE 30%<*siliceous fossil*	CALCAREOUS OOZE 30%<*calcareous fossil*

siliceous fossil; radiolarians, silicoflagellates, and sponge spicules
calcareous fossil: foraminifers and calcareous nannoplanktons

The framework of the sediment classification used in the previous work (NISHIMURA, 1981) is adopted in this work (Tab. VII-1).

Age estimations used in the discussions of this chapter are based on the micropaleontological works and paleomagnetic study of piston cores. The micropaleontology of radiolarians was preliminarily studied by the author on board. The micropaleontological study on some ichthyoliths and calcareous nannoplanktons is included in this chapter. The paleomagnetic study is reported by JOSHIMA (Chapter X in this cruise report).

In the GH80-5 Cruise, there are two surveyed areas, the detailed survey areas I and II. The lithologies of sediments are described on each surveyed area in following sections.

Sediments in the Detailed Survey Area I

This area is around 10°00'N and 174°40'W, north of the Magellan Trough, whose topography is characterized by rows of hills and troughs with axises of E-W to ESE-WNW trend. The topography of this area is shown in Fig. VII-1 including the summarized lithologies of piston cores. The description of piston cores and subcores of box cores are shown in Figs. VII-2 and -3 respectively. Water depth of the sampling localities of this area varies between 5,500 and 6,000 m.

Surface sediment of this area is composed of brown to dark brown siliceous fossil rich clay, except very dark brown pelagic clay of St1980 (P192) and St2011 (P200).

Piston corings were performed at 9 stations in this area. Core P193, P196 and P198 are composed of brown to dark brown siliceous fossil rich clay of the uppermost parts and dark brown pelagic clay of the rest. Core P195 and P199 are composed of brown siliceous fossil rich clay of the uppermost parts and very dark grayish brown zeolitic clay of the rest. Cores P192 and P200 are composed of pelagic clay of the uppermost parts and very dark grayish brown zeolitic clay of the rest. Core P197 is composed of brown siliceous fossil rich clay of the uppermost part, dark brown pelagic clay of the middle main part, and very dark grayish brown to dark

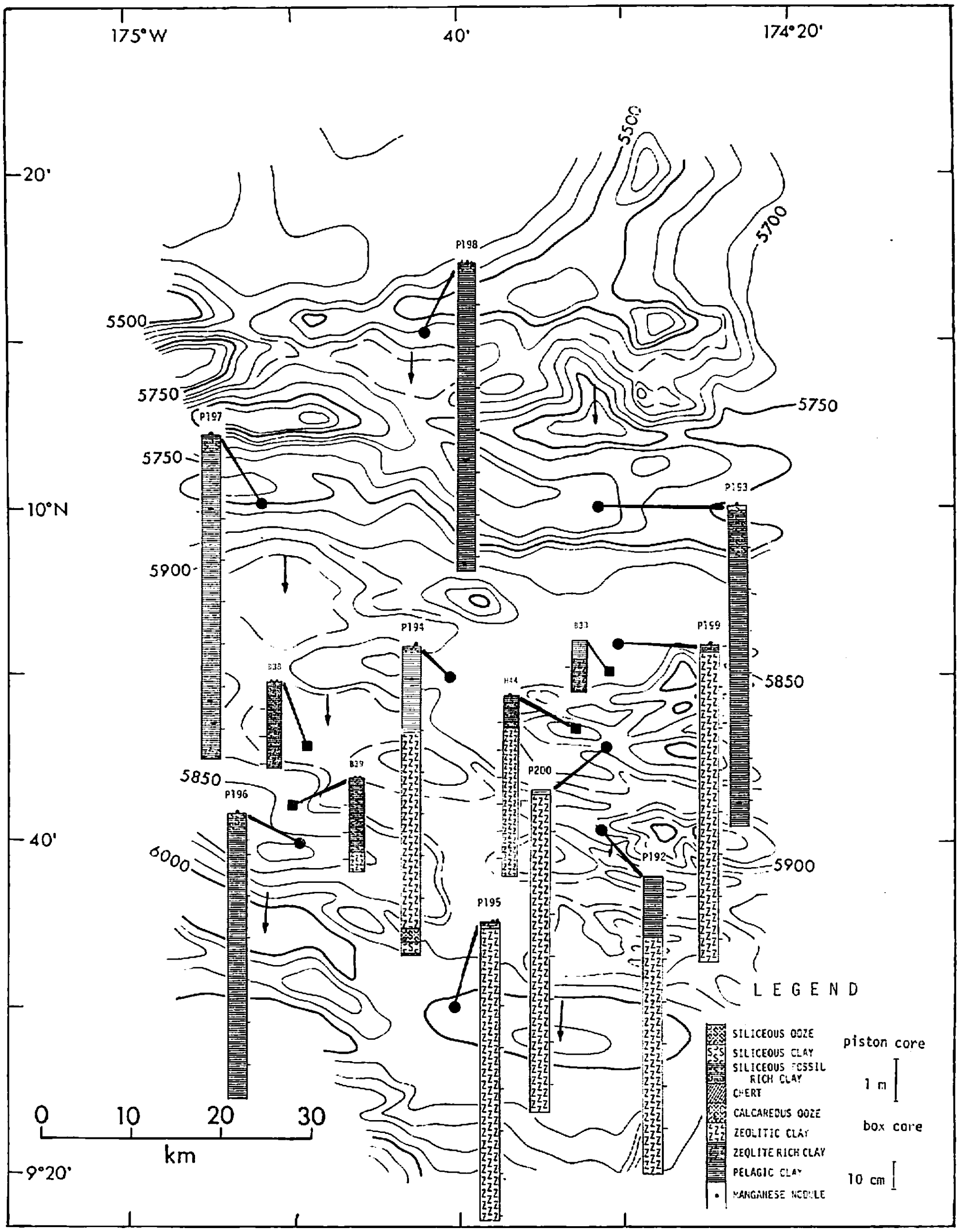

Fig. VII–1 Topography and outlined lithologies of piston cores of the Detailed Survey Area I. Box cores having zeolitic clay part and pilot core of H44 are also shown.

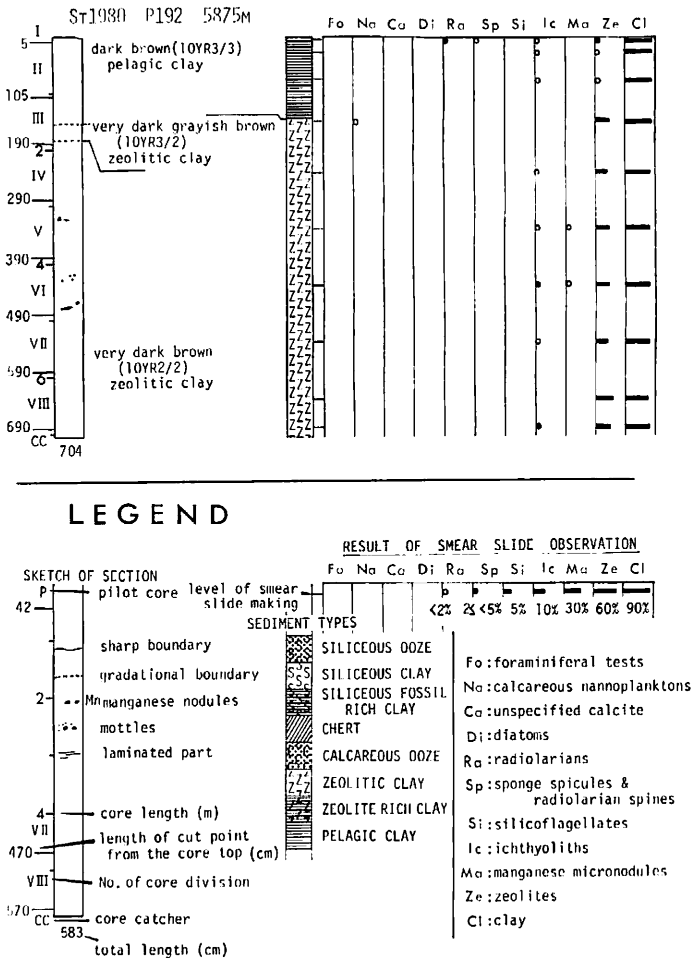

Fig. VII-2 (1)

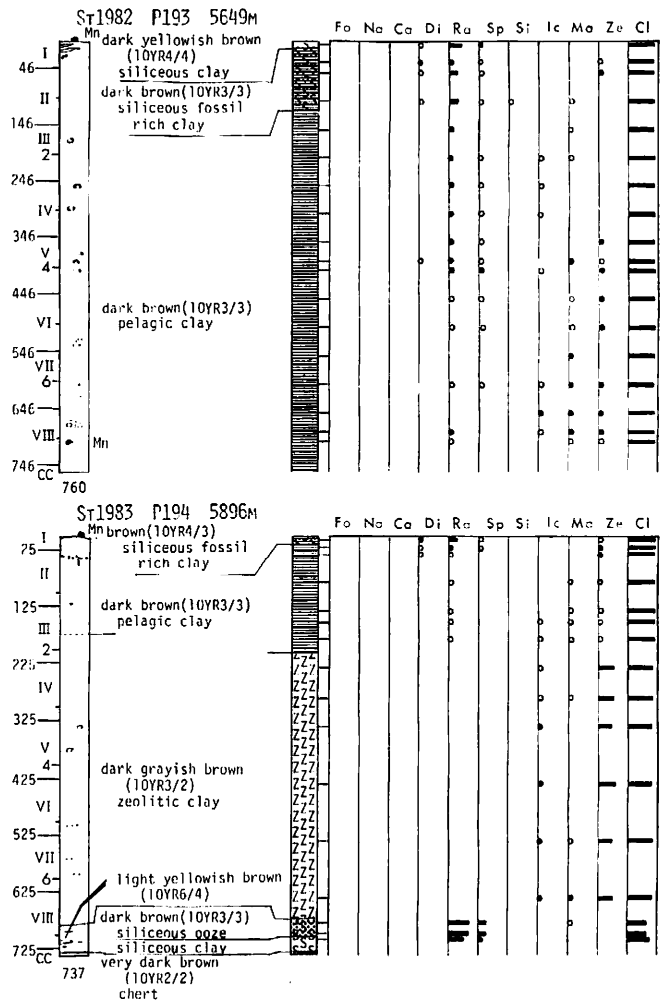

Fig. VII-2 (2)

Fig. VII-2 Descriptions of piston cores obtained from the Detailed Survey Area 1.

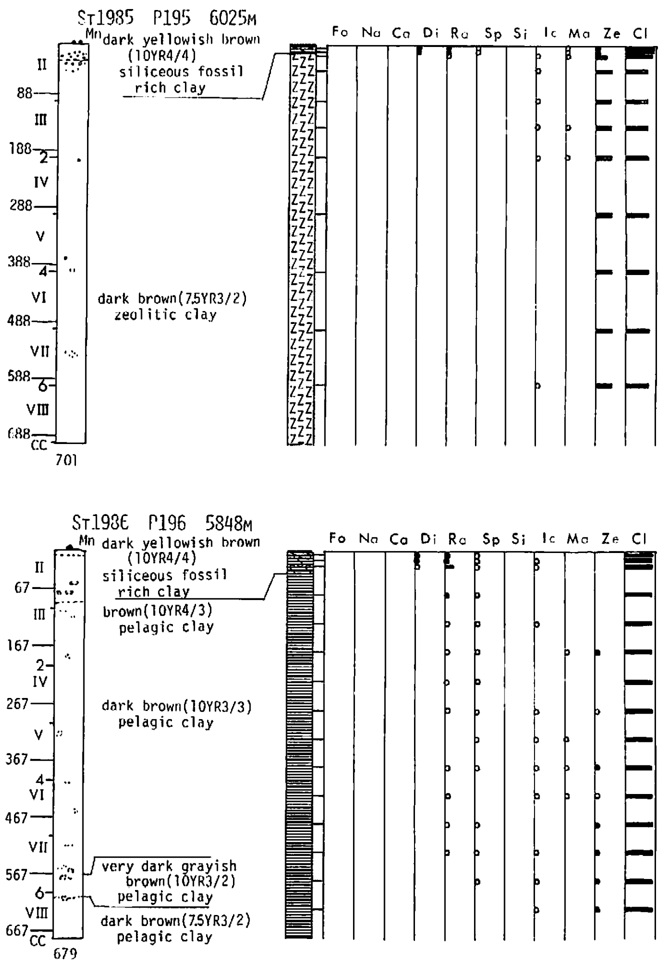

Fig. VII-2 (3)

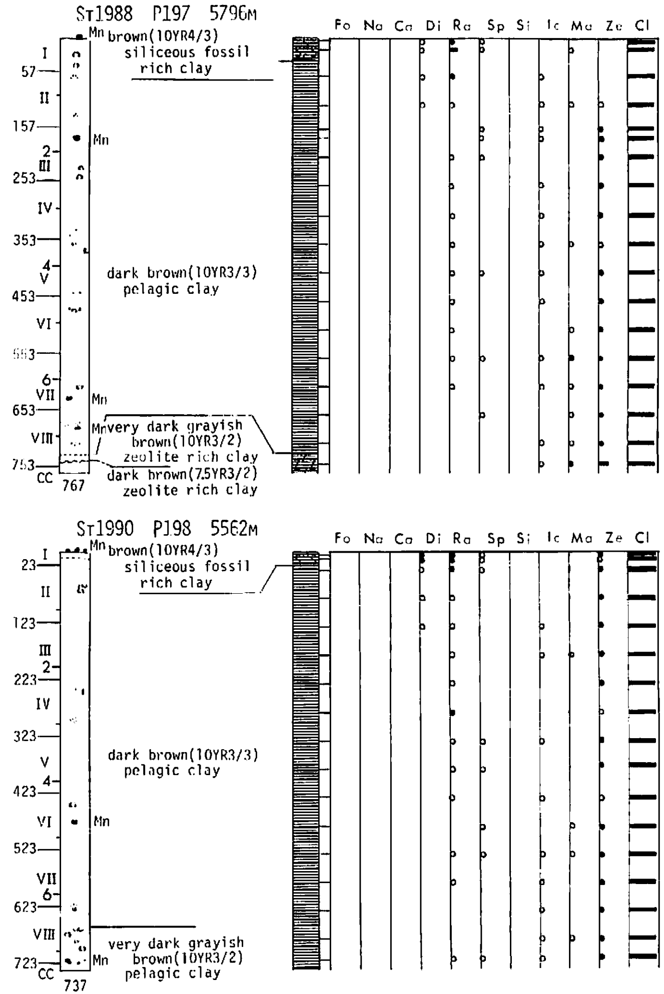

Fig. VII-2 (4)

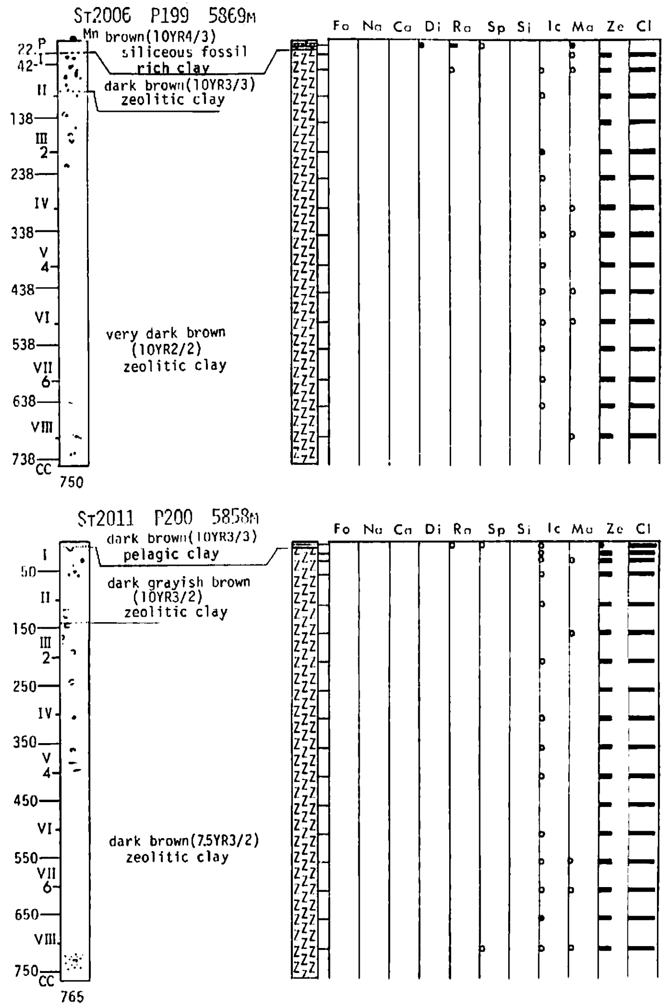

Fig. VII-2 (5)

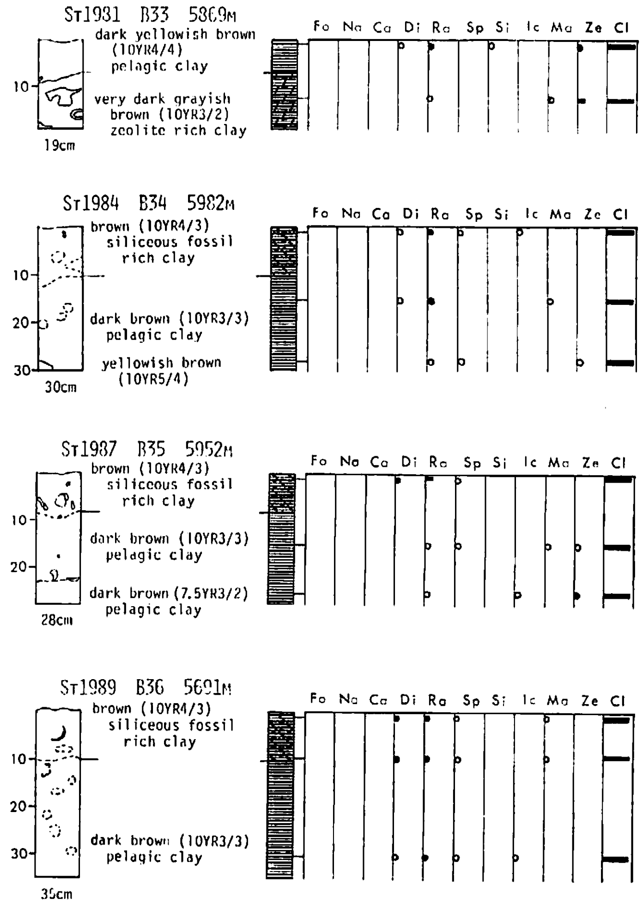

Fig. VII-3 (1)

Fig. VII-3 Descriptions of subcores of box cores obtained from the Detailed Survey Area 1.
Legend is the same as that of Fig. VII-2.

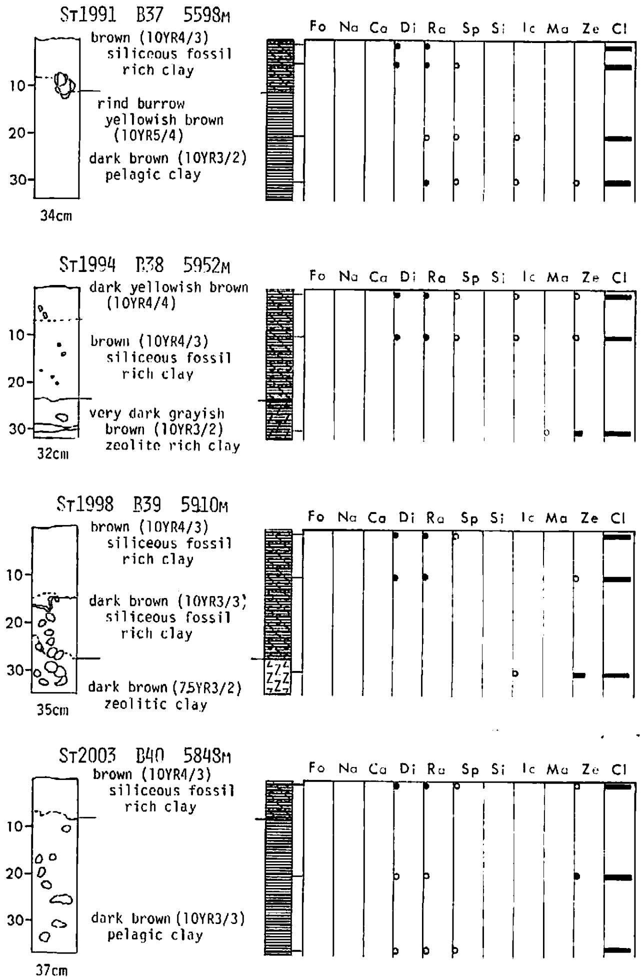

Fig. VII-3 (2)

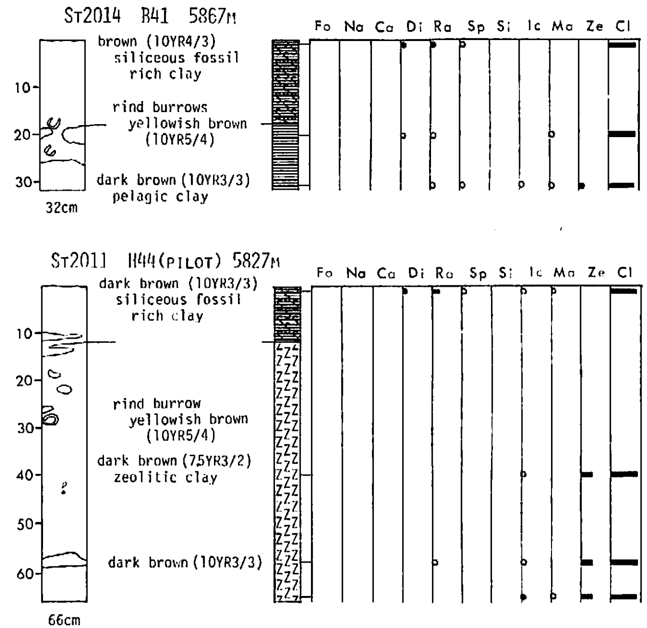

Fig. VII-3 (3)

brown zeolitic clay of the rest. Core P194 is complicated and represents a whole sequence of generalized succession of this area, mentioned later. This core is composed of brown siliceous fossil rich clay of the uppermost part, dark brown pelagic clay of the upper part, very dark grayish brown zeolitic clay of the middle to lower part, yellowish brown siliceous ooze and very dark siliceous clay of the lowest part, and very dark brown chert of the lowermost part of the core. This chert was found in the core catcher as a layer with 4 cm thickness. The surface of this chert etched with hydrofluoic acid shows that this is composed of abundant radiolarian tests and spines, few ichthyoliths, manganese micronodules, and brown matrix. These compositions are similar to those of the siliceous clay and ooze overlying the chert, hence this chert is thought to have been formed from the similar material to overlying siliceous sediments through diagenesis.

Manganese (macro-)nodules were found in the pelagic clay parts of Core P193, P197 and P198, except those from the tops of the piston cores.

Box corings were performed at 9 stations in this area. The successions observed in box cores are the same as that of the uppermost part of the piston cores of this area. Most of the box cores are composed of brown siliceous fossil rich clay of the upper part and dark brown pelagic clay of the lower part. The lower parts of box cores from three stations (St1981(B33), St1994(B38), and St1988(B39)) are composed of dark grayish brown zeolitic or zeolite rich clay.

The successions of the sediments of this area are summarized from the results of the piston corings and box corings, as follows.

1. The generalized succession of sediments is brown siliceous fossil rich clay, dark brown pelagic clay, dark grayish brown zeolitic clay, and dark brown to yellowish brown siliceous ooze, in descending order.

2. The thickness of each lithologic part varies at each sampling locality. The siliceous fossil rich clay and pelagic clay parts above the zeolitic clay part are tend to be thinner on and around the east-southern hills of this area.

Sediments in the Detailed Survey Area II

This area is a small area around 9°00'N, 174°00'W, south-east of the Detailed Survey Area I. The Magellan Trough with an axis of NW-SE trend is situated on the southern part of this area. The topography of this area is shown in Fig. VII–4, including the outlined lithologies of the piston cores. The descriptions of piston cores and subcores of box cores are shown in Figs. VII–5 and –6 respectively. Water depth of the sampling localities of this area varies between 5,800 and 6,300 m.

Surface sediment of this area is composed of brown siliceous fossil rich clay, as that of the Detailed Survey Area I.

Piston corings were performed at 8 stations in this area. Core P203 and P206 are composed of brown siliceous fossil rich clay of the uppermost part and dark brown pelagic clay of the rest. Core P208 is composed of brown siliceous fossil rich clay of the uppermost part and very dark grayish brown zeolitic clay of the rest. Core P202 is composed of brown siliceous fossil rich clay of the uppermost part, dark brown pelagic clay of the upper part, and very dark grayish brown zeolitic clay of the middle to lower part. Core P205 is composed of brown siliceous fossil

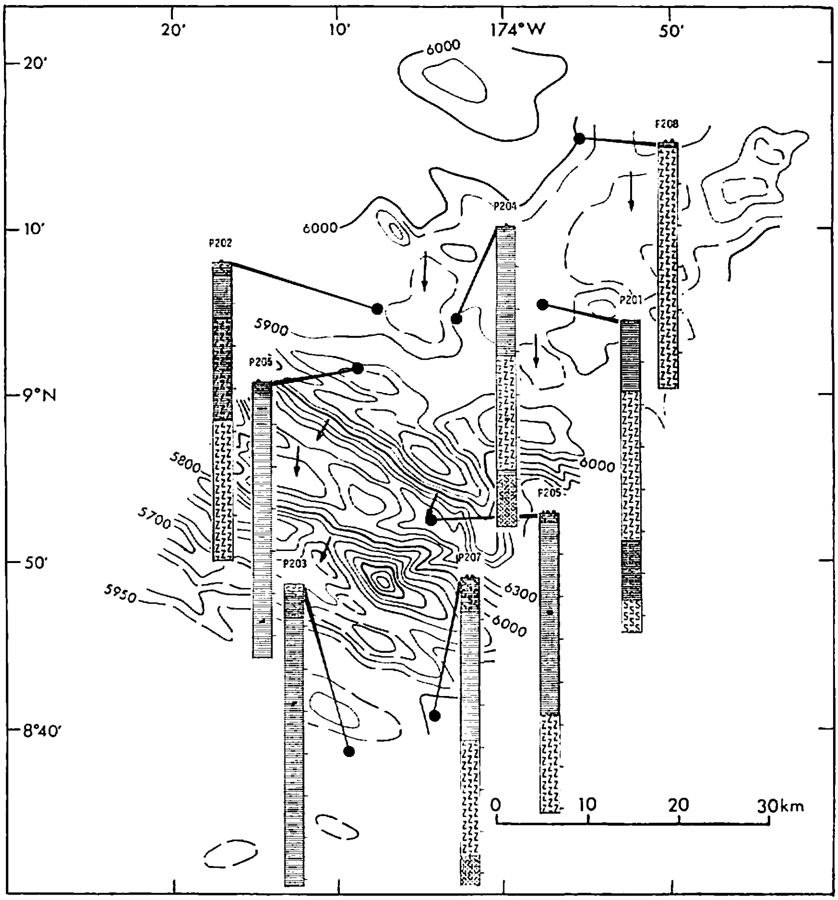

Fig. VII-4 Topography and outlined lithologies of piston cores of the Detailed Survey Area II. Legend is the same as that of Fig. VII-1.

rich clay of the uppermost part, dark brown pelagic clay of the upper to middle part, and very dark grayish brown zeolitic clay of the lower part. Core P201 is composed of brown siliceous fossil rich clay of the upper part, dark grayish brown zeolitic clay of the middle part, and dark brown siliceous fossil rich clay to siliceous clay of the lower part. Core P204 is composed of brown siliceous fossil rich clay of the uppermost part, dark brown pelagic clay of the middle to lower part, and yellowish brown siliceous ooze of the lowest part. Core P207 is composed of brown siliceous fossil rich clay of the uppermost part, dark brown pelagic clay of the upper to middle part, very dark grayish brown zeolitic clay of the middle to lower part, and pale brown calcareous ooze of the lowest part. At St2049(P207), a stratified layer is present below a very thin transparent layer on seismic records, and this stratified layer is thought to be a turbidite sequence (Tamaki, Chapter V in this cruise report). The lowest calcareous ooze part of Core P207 may correspond to the uppermost of this turbidite sequence.

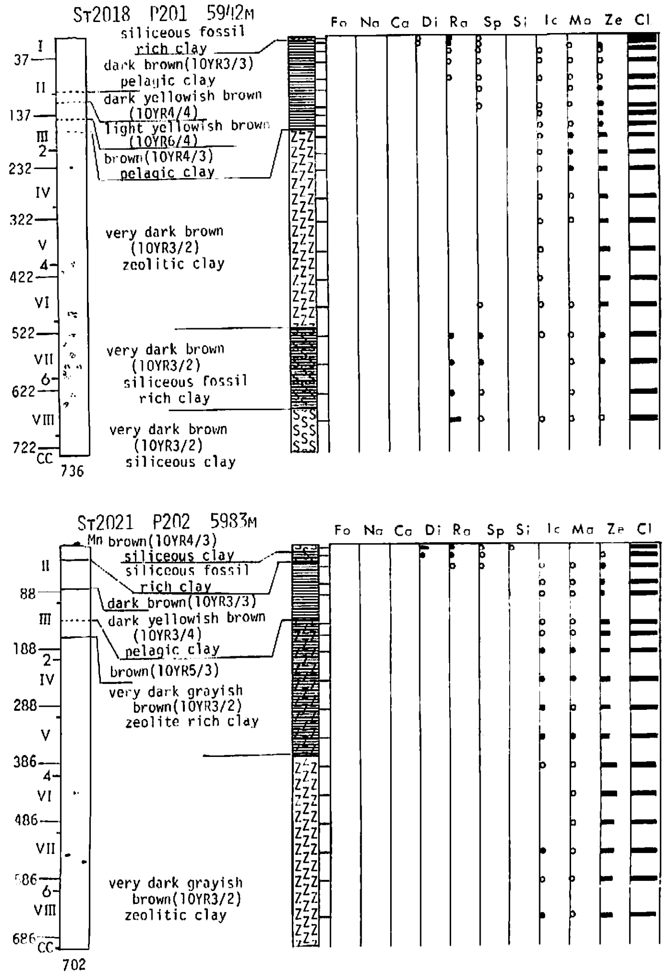

Fig. VII-5 (1)

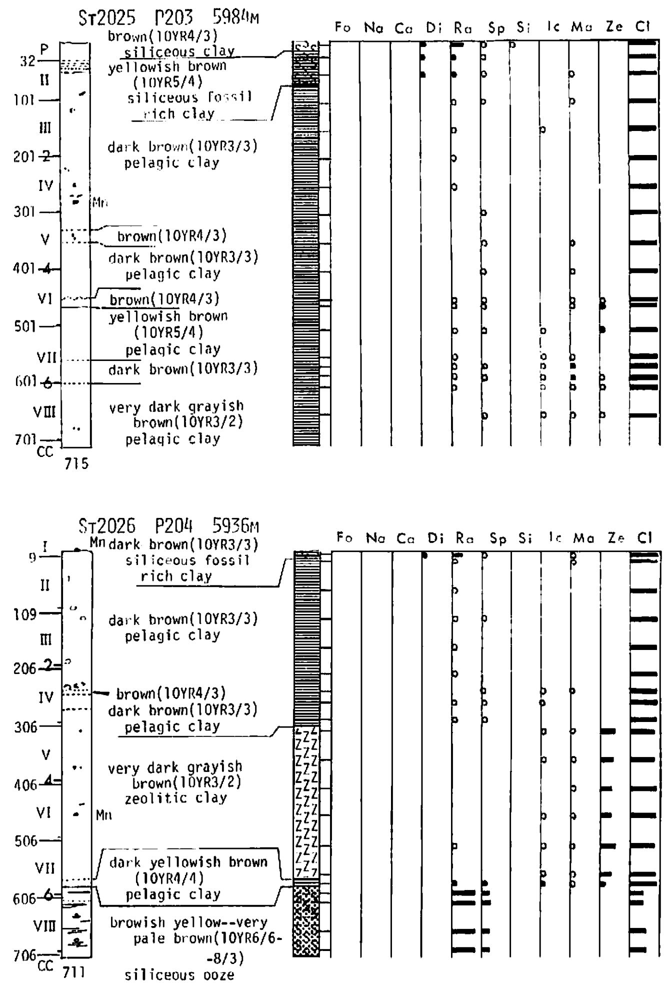

Fig. VII-5 (2)

Fig. VII-5 Descriptions of piston cores obtained from the Detailed Survey Area II.
Legend is the same as that of Fig. VII-2.

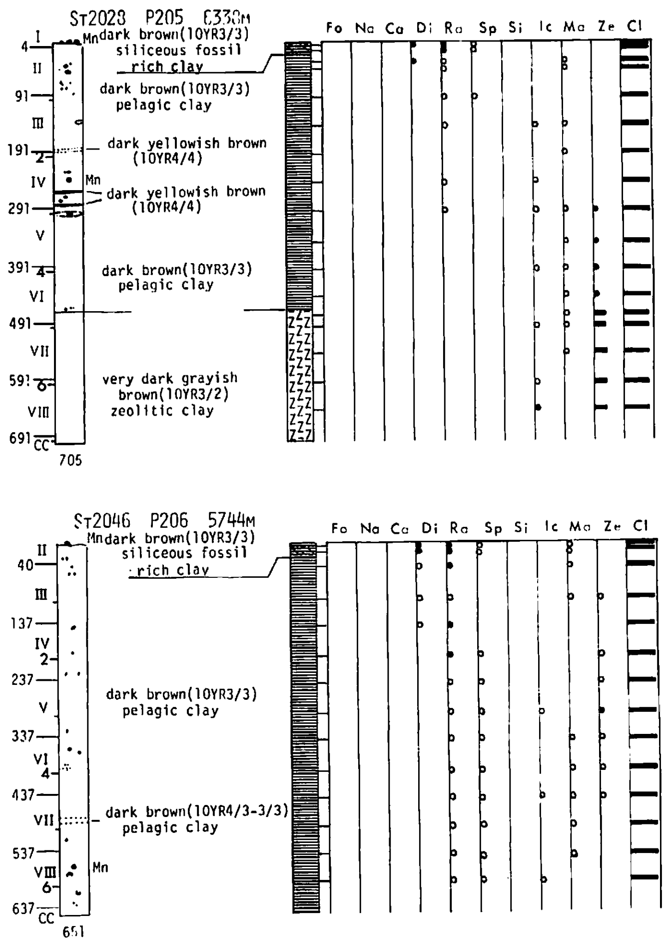

Fig. VII-5 (3)

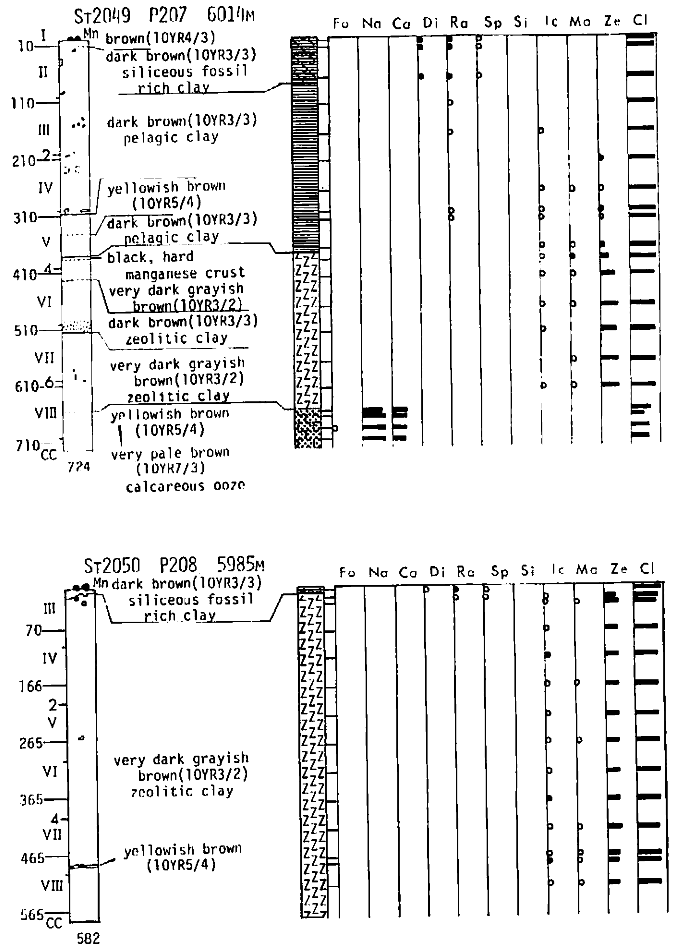

Fig. VII-5 (4)

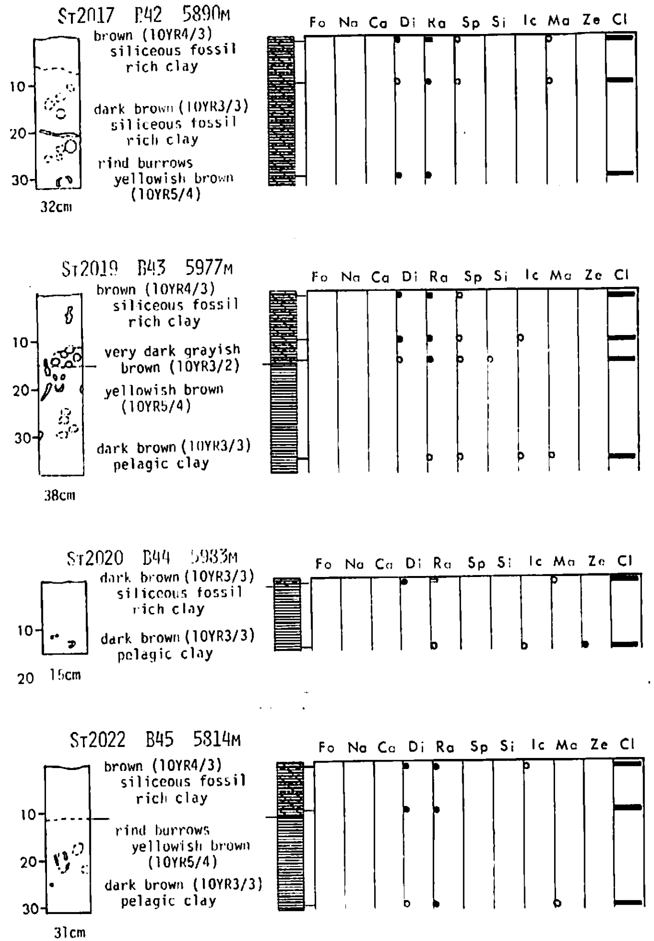

Fig. VII-6 (1)

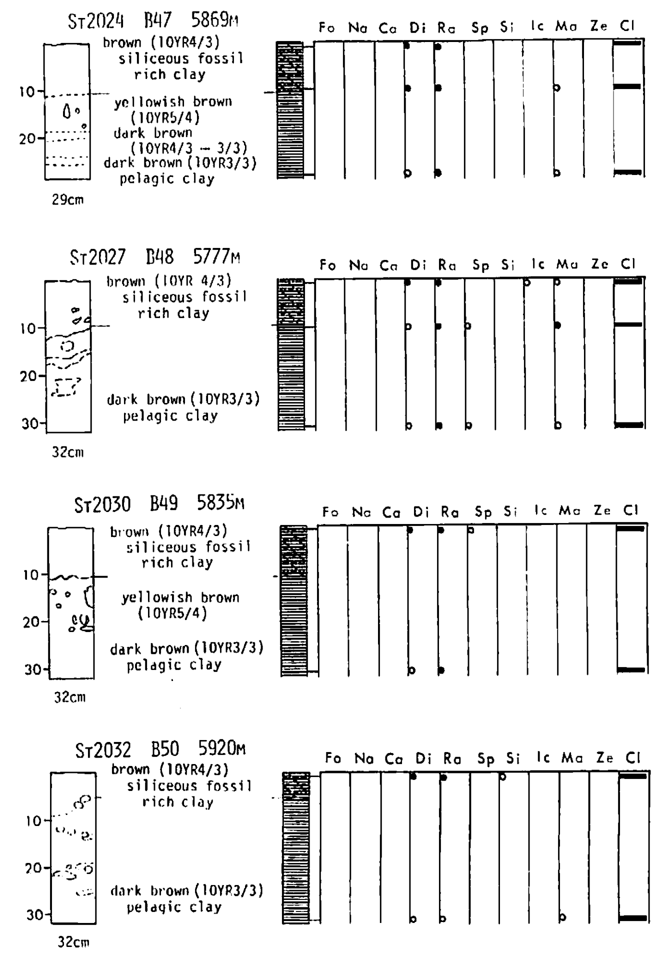

Fig. VII-6 (2)

Fig. VII-6 Descriptions of subcores of box cores obtained from the Detailed Survey Area II.
Legend is the same as that of Fig. VII-2.

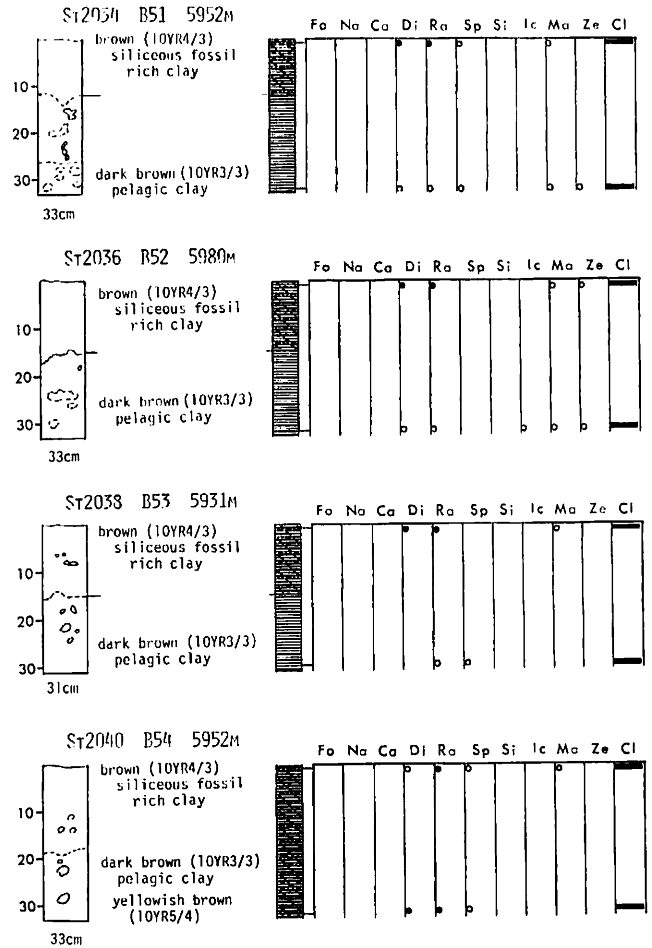

Fig. VII-6 (3)

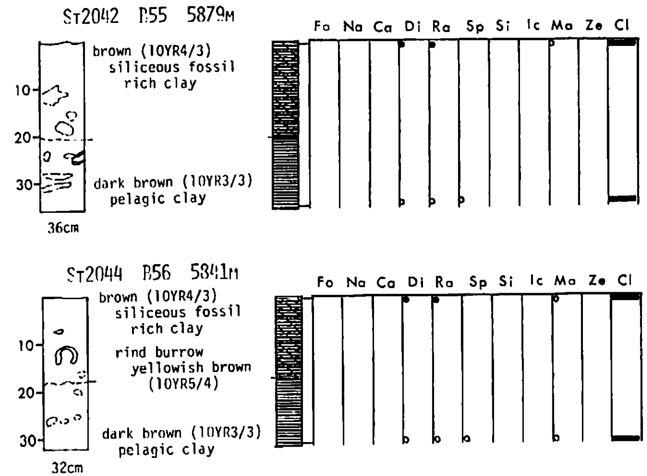

Fig. VII-6 (4)

Manganese (macro-)nodules were found in pelagic clay part of Core P203, P205 and P206 and zeolitic clay part of Core P204, in addition those from the tops of the cores.

Yellowish brown to brown decolorized parts are observed in the dark brown pelagic clay part of the cores in this area. The results of the chemical analysis (MITA, Chapter XIII in this cruise report) show that the contents of manganese and nickel in this decolorized part are smaller than those in the adjacent pelagic clay.

Box corings were performed at 15 stations in this area. The successions observed in box cores are the same as that of the uppermost part of the piston cores in this area. All the box cores are composed of brown siliceous fossil rich clay and/or dark brown pelagic clay.

The successions of the sediments of this area are summarized from the data of the piston cores and box cores, as follows.

1. The generalized succession of sediments is brown siliceous fossil rich clay, dark brown pelagic clay, and dark grayish brown zeolitic clay, in descending order.
2. Various types of sediments are observed in the lowest part of the cores (for example, siliceous ooze of Core P204, siliceous clay of Core P201, and calcareous ooze of Core P207).
3. The thickness of the upper lithologic unit (siliceous fossil rich clay and pelagic clay parts) is tend to be thinner in the northern and eastern parts of this area.
4. Manganese nodules are found in the pelagic clay and zeolitic clay part in the piston cores in addition to those on the surfaces.
5. Decolorized parts are observed in the pelagic clay parts of this area.

Remarks on occurrence of sedimentary components

Some features of occurrence of each sedimentary component related to the sediment types, mainly on the smear slide observation data, are given below.

Foraminifers and calcareous nannoplanktons are not observed in the surface sediment samples of this area, because the Calcium Carbonate Compensation Depth of this area is present shallower than 5,100 m, judged from the result of TAKAYANAGI *et al.* (1982). The lowest part of Core P207 is composed of calcareous (nanno-)ooze, which contains abundant calcareous nannoplanktons and a few fragmental and small tests of planktonic foraminifers. This calcareous ooze is considered to have deposited as a turbidite, as mentioned before. This ooze was primarily deposited on the high relief above the CCD of that time.

Diatoms and silicoflagellates are rarely observed in siliceous clay and siliceous fossil rich clay.

Radiolarians are commonly observed in siliceous clay and siliceous fossil rich clay of the upper part of the cores, and abundantly observed in siliceous ooze of the lower part of the successions. Radiolarian tests are rare in the pelagic clay part, and they are poorly preserved.

Sponge spicules and radiolarian spines are observed in the same manner as radiolarian tests, though the content of them is smaller than that of radiolarians.

Ichthyoliths are often observed in the pelagic clay and zeolitic clay part of the cores, and rarely observed in the other lithologic parts.

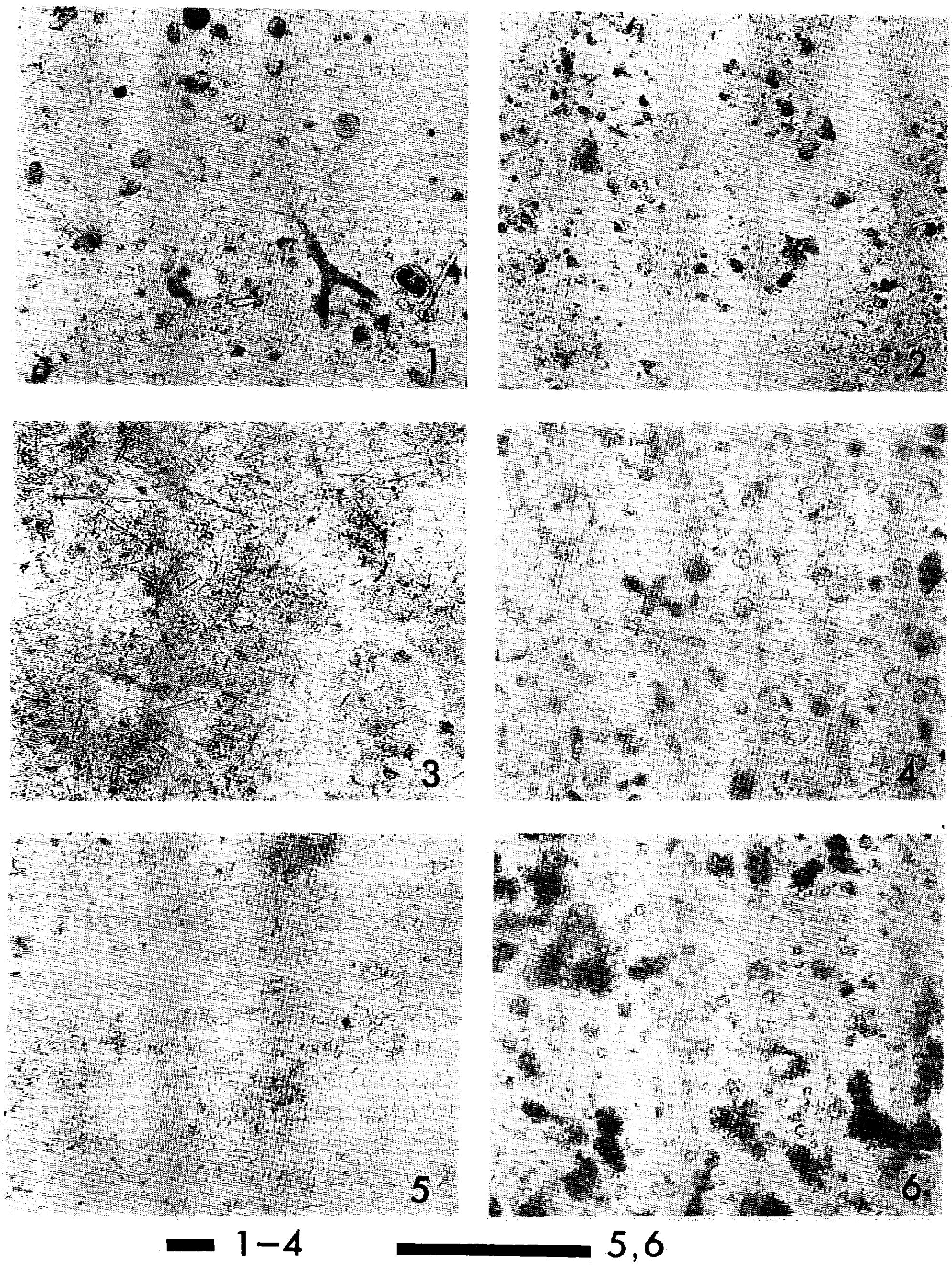

Fig. VII–7 Photographs of smear slides of sediments.
Scale bars show 200 μm.

1. Siliceous fossil rich clay, Core P194, 0 cm.
2. Pelagic clay, Core P196, 427 cm.
3. Siliceous ooze, Core P194, 685 cm.
4. Siliceous ooze, Core P204, 666 cm.
5. Zeolitic clay, Core P199, 448 cm.
6. Calcareous ooze, Core P207, 690 cm.

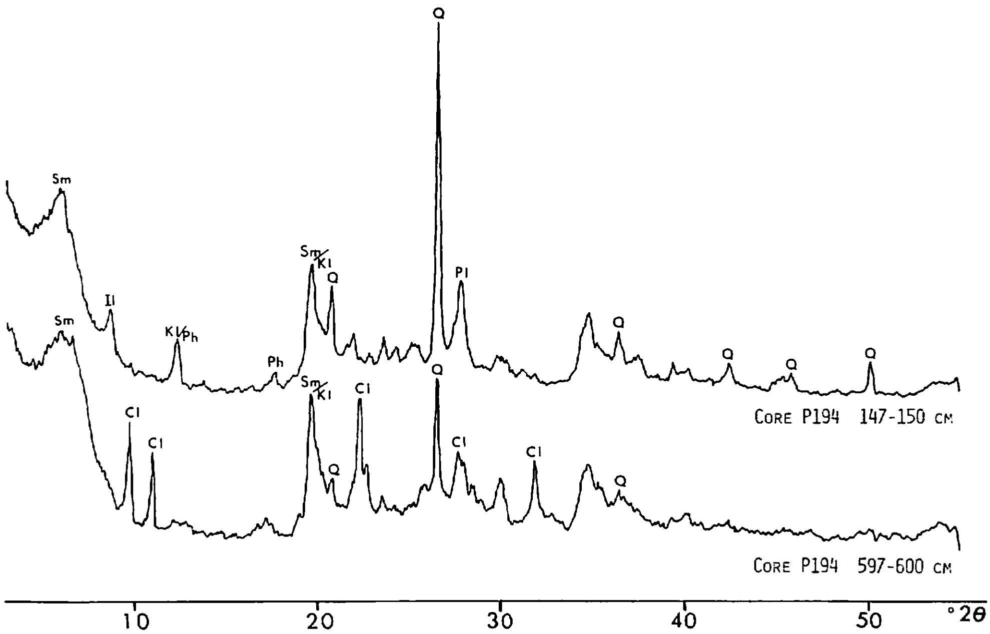

Fig. VII–8 Results of X-ray diffraction analysis on sediment samples of Core P194. This analysis were done by NAKAO, an editor of this cruise report. Q; quartz Pl; plagioclase Kl: kaolin Il; illite Sm; smectite Ph; phillipsite Cl; clinoptilolite

Zeolites are commonly observed in the cores, as a major component of zeolitic clay and a minor component of pelagic clay. Pelagic clay part overlies zeolitic clay part as mentioned in previous sections. Preliminary analysis of the X-ray diffraction was performed on the bulk sediment samples from the two parts of Core P194. The results show that the pelagic clay contains phillipsite and that the zeolitic clay contains clinoptilolite (Fig. VII–8). And then cross-shaped zeolite crystals which are considered to be phillipsite are sometimes observed in the smear slides of the pelagic clay. On the contrary zeolite crystals as a major component of the zeolitic clay part, are tiny prismatic forms in the smear slides. Although the X-ray diffraction analyses were performed on only two samples, it is probably concluded that zeolite in the pelagic clay part is composed of phillipsite and that zeolite in the zeolitic clay part is mainly composed of clinoptilolite. This phenomena show good correspondence to the results of STONECIPHER (1976), which suggest that clinoptilolite generally occurs from the sediments older and lower than the sediments with phillipsite.

Age assignments of some samples

Age assignments from the magnetic studies on core sequences are outlined in Figs. VII–9 and VII–10 (JOSHIMA, Chapter X in this cruise report).

Radiolarians of siliceous ooze and clay of lower parts of Cores P194, P201 and P204 were preliminarily studied. Siliceous ooze of Core P194 yields *Eusyringium fistuligerum* EHRENBERG, *Podocyrtis chalara* RIEDEL and SANFILIPPO, *P. goetheana*

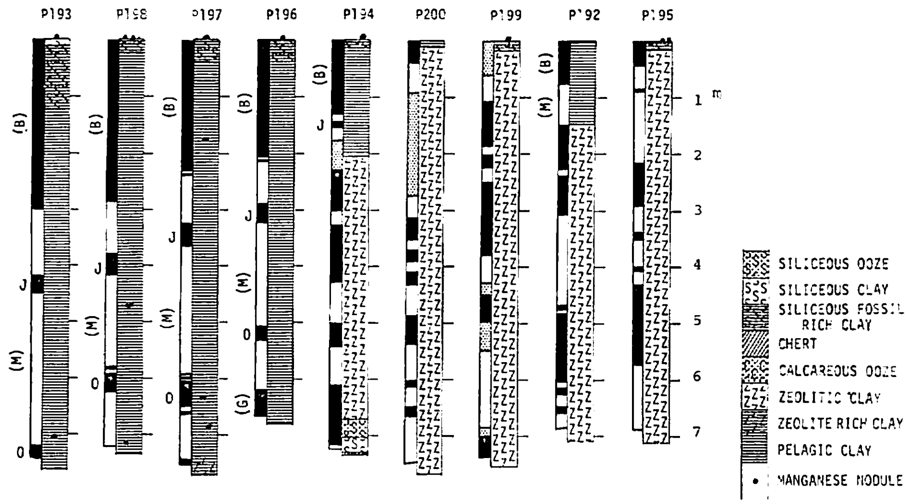

Fig. VII-9 Simplified results of magnetic study on piston cores in the Detailed Surveyed Area I.

Magnetic measurements were done by JOSHIMA (this cruise report).

Left columns show the magnetic polarity of sediments. Black shows normal polarity, white does reversed polarity, and dotted part does intermediate or unstable polarity.

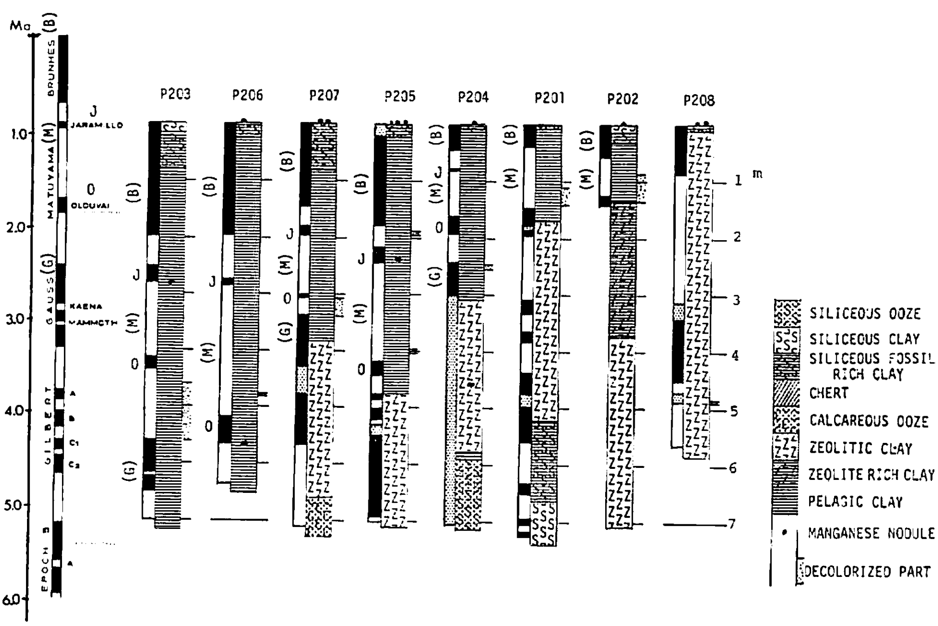

Fig. VII-10 Simplified results of magnetic study on piston cores in the Detailed Survey Area II.

Magnetic measurements were done by JOSHIMA (this cruise report).

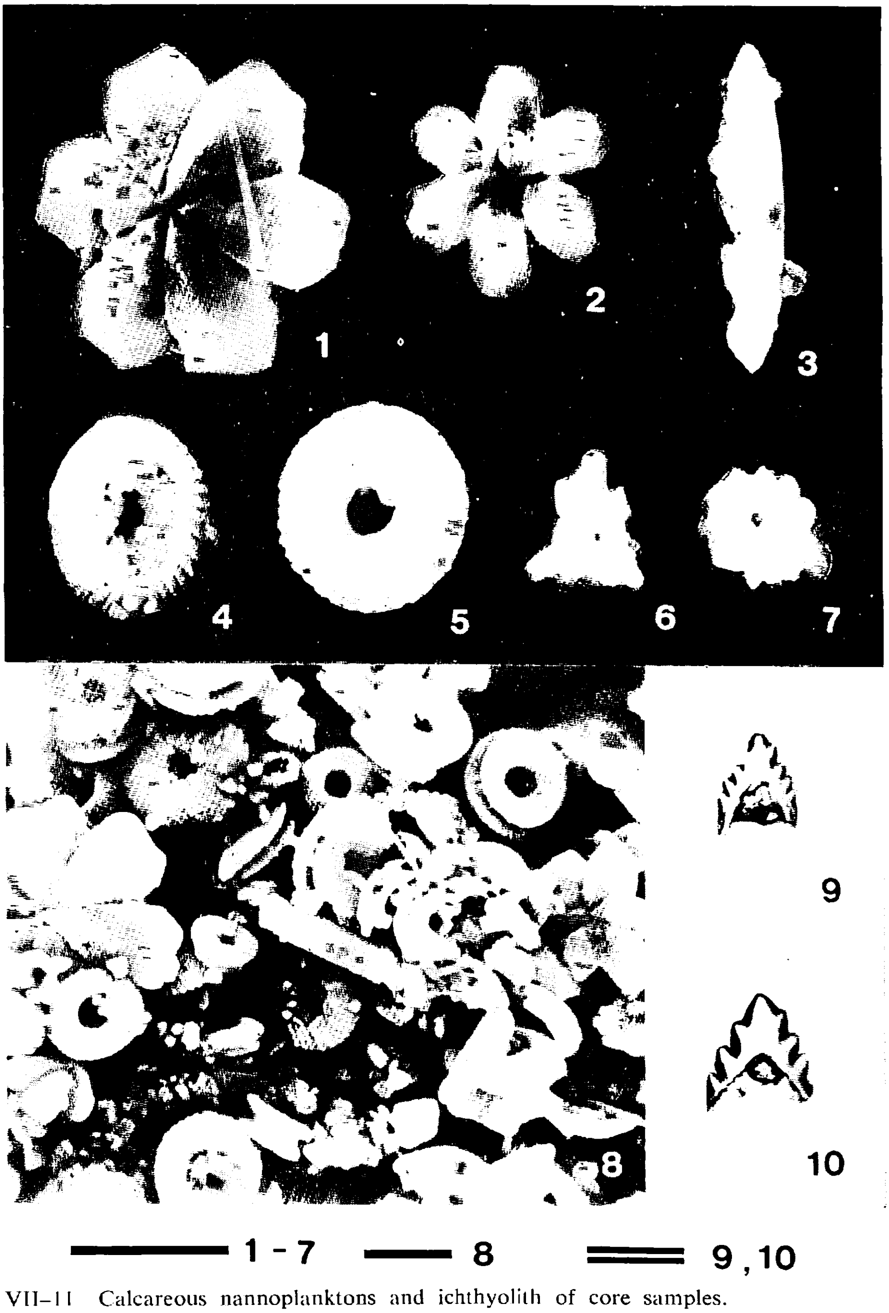

Fig. VII–11 Calcareous nannoplanktons and ichthyolith of core samples.
Single-scale bars show 4 μm and double-bar shows 200 μm.
All calcareous nannoplanktons are obtained from the calcareous ooze of Core P207 (702–705 cm). Ichthyolith is obtained from the zeolitic clay of Core P197 (557–600 cm).

1. *Discoaster deflandrei* BRAMLETTE and RIEDEL
2. *Discoaster deflandrei* BRAMLETTE and RIEDEL
3. *Triquetrorhabdulus carinatus* MARTINI
4. *Cyclicargolithus floridanus* (ROTH and HAY)
5. *Cyclicargolithus floridanus* (ROTH and HAY)
6. *Sphenolithus moriformis* BRONNIMANN and STRADNER
7. *Sphenolithus moriformis* BRONNIMANN and STRADNER
8. Calcareous nanno-ooze
9. Ichthyolith, '*Small triangle crenata margin*'
10. Ichthyolith, '*Small triangle crenata margin*'

(HAECKEL), *Thyrsocyrtis triacantha* EHRENBERG, and *Lithochyrtis vespertilio* EHRENBERG. This assemblage assigns the late Eocene. Siliceous clay of Core 201 yields *Ommatartus antepenultimus* RIEDEL and SANFILIPPO and shows the late Miocene. Siliceous ooze of Core P204 shows the early- middle Eocene assemblage, which contains *Amphicraspedum murrayanum* HAECKEL and *Phomocyrtis striata exquisita* FOREMAN.

Zeolitic clay part of Core P194 was examined for the ichthyolith biostratigraphy. The analysis was performed on the whole sequence of Core P194 at an interval of 50 cm. From the residue sediment samples sieved on a screen with 63 μm openings, ichthyoliths were picked up. Ichthyoliths were constantly found throughout the zeolitic clay part. The lower part of the zeolitic clay (447–600 cm) yields '*Small triangle crenata margin*' type ichthyoliths, which are small but easily distinguished by their peculiar shapes (Fig. IX–11). This type has the range from the early Eocene through the early Oligocene (DOYLE and RIEDEL, 1979). This age assignment and the radiolarian assemblage of the siliceous ooze underlying this zeolitic clay part, restrict the age of the lower part of the zeolitic clay part between the late Eocene and early Oligocene and suggest that no large age difference exists between the zeolitic clay and the siliceous ooze parts.

A chert layer obtained in the core catcher of Core P194 is radiolarian chert as mentioned before. The radiolarian tests observed on the surface etched by hydrofluoic acid are so delicate that they are soluble in hydrofluoic acid with brown matrix and that no free specimen was obtained. Very few radiolarians on the surface are identified. They are *Thyrsocyrtis tetracantha* (EHRENBERG) etc., which indicate the Eocene age as the same as that of the siliceous ooze overlying this chert.

Calcareous ooze of Core P207 are mainly composed of calcareous nannoplankton tests. The assemblage mainly composed of *Discoaster deflandrei* BRAMLETTE and RIEDEL, suggests the Oligocene to the early Miocene age to the calcareous ooze (Fig. VII–11).

Summary

Because the two surveyed areas are small and adjacent each other, and similar lithologic successions are observed in the core sequences obtained from the two areas, here two areas are considered in a lump to construct the sedimentary history.

The schematic sequence with geologic age is compiled in Fig. VII–12, based on the all data of the sediment cores. The generalized lithologic succession of the two areas is roughly divided into four parts, siliceous fossil rich clay, pelagic clay, zeolitic clay and siliceous ooze in descending order. In terms of the micropaleontology of radiolarians, the uppermost siliceous fossil rich clay part yields Recent radiolarian assemblage. And the paleomagnetic study of the cores shows that the siliceous fossil rich clay and pelagic clay parts correspond to the standard magnetic pattern from the Brunhes Epoch to the older epochs or events. Some cores shows continuous sedimentation down to the Gauss Epoch. The lithological change between the two parts is gradual. These phenomena imply that the upper siliceous fossil rich clay continues to the deposition of the pelagic clay without time gap. In the zeolitic clay part, the magnetic intensity is weak and magnetic patterns are complicated and shows

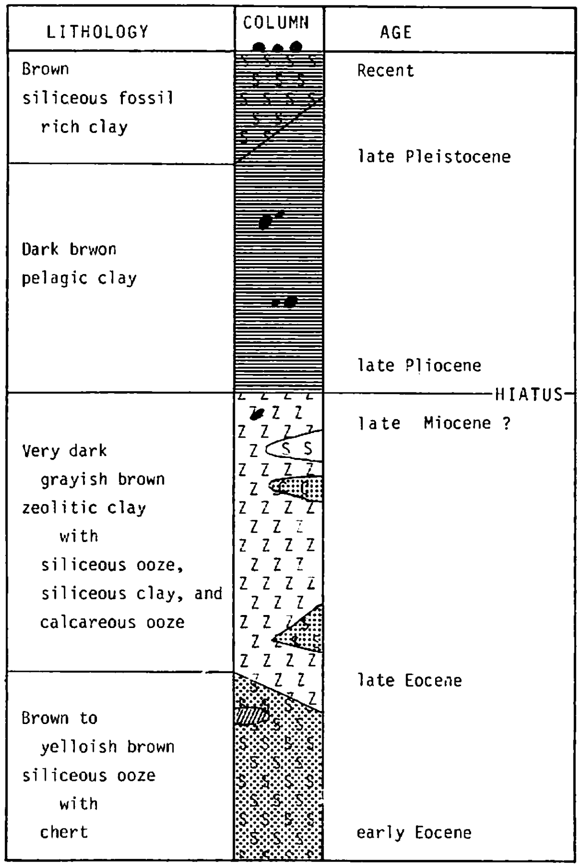

Fig. VII–12 Schematic sequence of the surveyed area.
Legend is the same as that of the lithology of Fig. VII–2.

no continuity from the upper pelagic clay part. The lowest siliceous ooze and siliceous clay of some cores are of the early Eocene to the late Miocene age. In Core P194, the lithologic change between the zeolitic clay and siliceous ooze parts is conspicuous, but the continuity between the two parts is suggested by the absence of a remarkable age difference between the two parts, as mentioned in the previous section. Then, the zeolitic clay had been deposited after the late Eocene (the middle Eocene?), and sometimes siliceous clay or siliceous ooze were deposited through the time of zeolitic clay deposition. It is considered that there is a large hiatus between the upper lithologic unit (siliceous fossil rich clay and pelagic clay parts) and the lower lithologic unit (zeolitic clay part including siliceous ooze, siliceous clay and calcareous ooze). This hiatus lacks the sediments from the middle Miocene to the lower Pliocene at least.

The geological history of this area are summarized as follows, based on the lithologic succession and some other data.

(1) In Eocene age, this area was situated in equatorial high productivity province of biogenic opal and siliceous ooze composed of radiolarian tests were deposited below the CCD of that time. Some parts of the siliceous sediments have changed to chert

through diagenesis.

(2) After the Oligocene through the Miocene, northwest ward plate motion (VAN ANDEL *et al.*, 1975) led this area out of high productivity province, where clay was deposited. Sometimes, the extension of high productivity province, which may be related to the increased siliceous organism productivity in equatorial area shown by LEINEN (1979), caused the deposition of siliceous sediments. And in south of the Magellan Trough, calcareous ooze were deposited as a turbidite originated from the high relief part. In slow depositional conditions, zeolites or their precursors were precipitated.

(3) After the late Miocene, strengthened bottom water current made no deposition and/or erosional condition on this area, especially in the center of the sur-

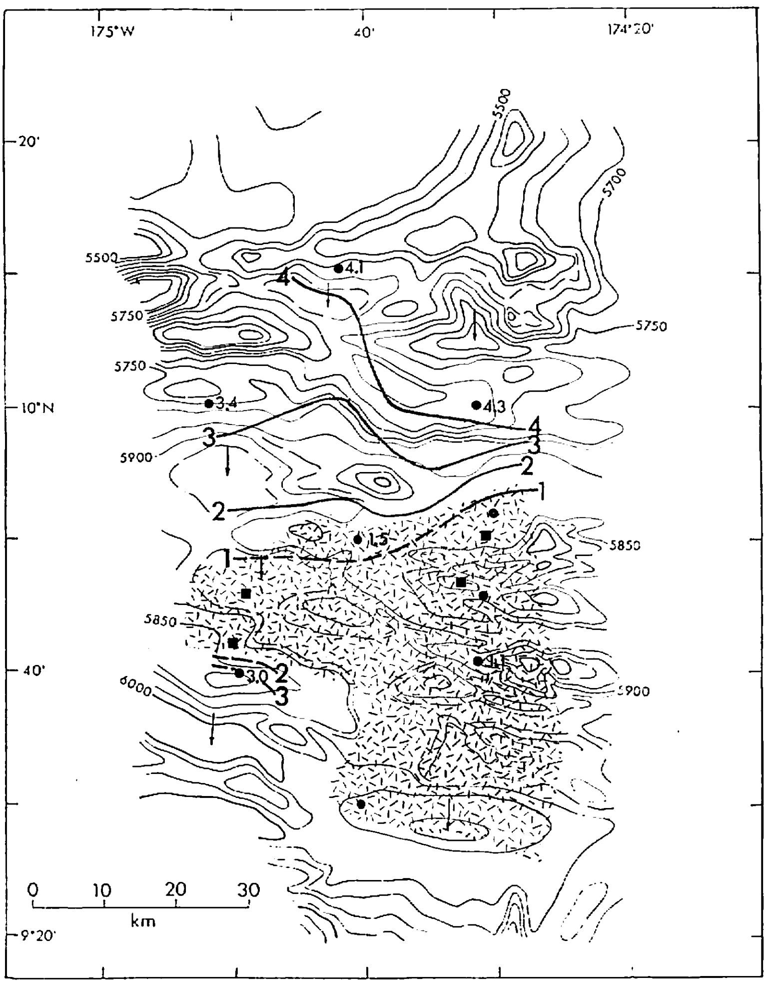

Fig. VII-13 Variation of sedimentation rate in the Detailed Survey Area I.
Numbers show average sedimentation rates (m/Ma) of the Brunhes Epoch inferred from the paleomagnetic study of the cores. Hatched part shows distribution of zeolitic clay part in piston core and box core sections.

veyed area.

(4) After the late Pliocene, pelagic clay was deposited in this area, and recently siliceous fossil rich clay has been deposited. Pelagic clay may have been made from siliceous fossil rich clay through the process of the dissolution of siliceous fossil through diagenesis.

The abundance and types of manganese nodules are conspicuously changed in the surveyed area. The samplings of bottom sediments by a piston corer are so sporadic that exact relation between the sediment sequences and manganese nodule occurrences are not given. Then, only some features related to manganese nodules are comprised below.

1. In piston core sections, buried manganese nodules are found from the pelagic clay part, except the occurrence in the zeolitic clay part of Core P204. Almost all horizons of buried manganese nodules in the pelagic clay are in the Matuyama Reversed Epoch (Figs. IX–9 and –10).

2. Roughly speaking, the area with r-type nodules coincides with the area with thin thickness of the upper lithologie unit (siliceous fossil rich clay and pelagic clay parts) (Figs. IX–1 and –4). This phenomena do not coincide with that the area with thinner upper sequence (mainly composed of Quaternary sediments) has s-type nodules in the GH79–1 detailed survey area in the northeastern margin of the Central Pacific Basin (MIZUNO *et al.*, 1980).

3. The area with larger sedimentation rate of the upper lithologic unit (2–4 m/

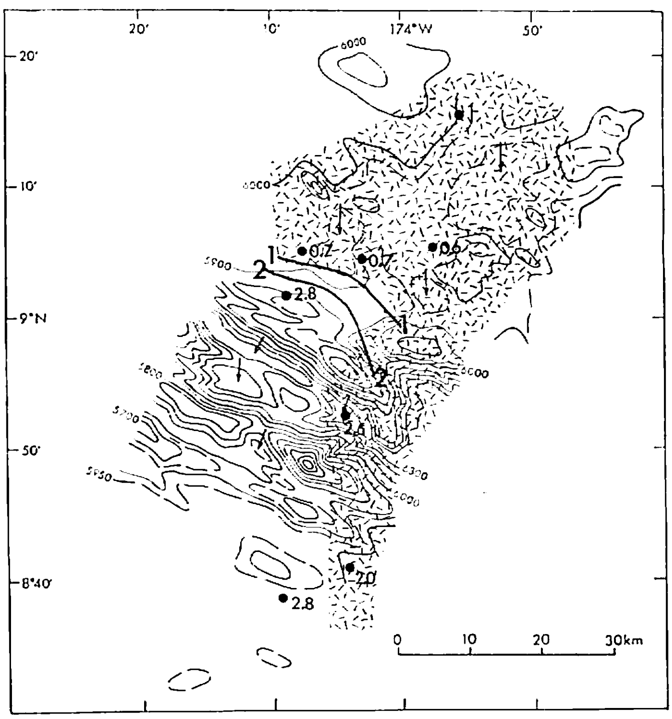

Fig. VII–14 Variation of sedimentation rate in the Detailed Survey Area II.

Ma) coincides the area with distribution of s-type nodules, and the area with smaller sedimentation rate of the upper lithologic unit (smaller than 1 m/Ma) does the area with r-type nodules. This phenomena are observed especially in the Detailed Survey Area I (Figs. VII–13 and –14). This is also inconsistent with the results in the GH79–1 detailed survey area.

4. Decolorized part with reaching of manganese in the pelagic clay part are observed in the piston cores obtained from the Detailed Survey Area II. Most of these parts are in the Matuyama Reversed Epoch (Fig. VII–10).

References

DOYLE, P. S. and RIEDEL, W. R. (1979) Ichthyoliths: present status of taxonomy and stratigraphy of microscopic fish skeletal debris. *SIO Reference* no. 79–16, p. 1–231. Univ. California.

LEINEN, M. (1979) Biogenic silica accumulation in the central equatorial Pacific and its implications for Cenozoic paleoceanography: summary. *Geol. Soc. America Bull.*, part I, v. 90, p. 801–803.

MIZUNO, A., MIYAZAKI, T., NISHIMURA, A., TAMAKI, K., and TANAHASHI, M. (1980) Central Pacific manganese nodules and their relation to sedimentary history. *Proc. Offshore Technology Conference in Houston*, May 5–8, 1980, p. 331–340 (OTC 3830).

NISHIMURA, A. (1981) Deep-sea sediments in the GH79–1 area; Their geological properties. *Geol. Surv. Japan Cruise Rept.*, no. 15, p. 110–142.

STONECIPHER, S. A. (1976) Origin, distribution and diagenesis of phillipsite and clinoptilolite in deep-sea sediments. *Chem. Geol.*, v. 17, p. 307–318.

TAKAYANAGI, Y., SAKAI, T., ODA, M., and HASEGAWA, S. (1982) Micropaleontology of piston cores, Wake to Tahiti. *Geol. Surv. Japan Cruise Rept.*, no. 18, p. 238–263.

VAN ANDEL, T. H., HEATH, G. R., and MOORE, T. C. (1975) Genozoic history and paleoceanography of the Central Equatorial Pacific Ocean. *Geol. Soc. America Mem.*, no. 143, p. 1–134.